ISSN 1028-334X, Doklady Earth Sciences, 2024, Vol. 516, Part 1, pp. 763–767. © Pleiades Publishing, Ltd., 2024.
ISSN 1028-334X, Doklady Earth Sciences, 2024. © Pleiades Publishing, Ltd., 2024.

OCEANOLOGY

Transformations of Bottom Pressure Variations Generated by Marine Infragravity Waves into Displacements of the Upper Layer of the Earth's Crust: Quantitative Assessment

Academician **G. I. Dolgikh**[a], **S. S. Budrin**[a,*], **and S. G. Dolgikh**[a]

Received November 29, 2023; revised January 11, 2024; accepted January 15, 2024

Abstract—Transformations of bottom pressure variations generated by infragravity waves into displacements of the upper layer of the Earth's crust have been quantitatively assessed based on the experimental data obtained with a laser meter for hydrospheric pressure variations and two laser strainmeters. The relationship between the coefficient of bottom pressure transformation into elastic vibrations of the Earth's crust and the infragravity wave period has been determined.

Keywords: infragravity waves, microseisms, laser meter for hydrosphere pressure variations, laser strainmeter

DOI: 10.1134/S1028334X24600841

The natural seismic noise in the upper layer of the Earth's crust is relatively highly variable and ranges from a few seconds to tens of minutes. This range can be conditionally divided into several segments corresponding to periods of characteristic physical processes. The major phenomena that generate natural seismic noise, especially in the coastal areas, are microseisms of the first and second types caused by progressive and standing sea gravity waves [1] with a range from 2 to 20 s. The periods of the microseisms of the second type are equal to those of progressive sea waves, while periods of microseisms of the first type correspond to those of standing sea waves which are half as long as the progressive wave periods [2]. However, the period range of more than 20 s is the most interesting in terms of research and the least studied. It is due to the influence of infragravity sea waves on the upper layer of the Earth's crust.

According to [3], these infragravity waves result from the reflection of wind waves and swell from the shore, as well as from nonlinear interaction of wind waves and swell in the open ocean. Pressure fluctuations caused by infragravity waves were identified as an important source of microseismic noise on the ocean floor [4]. Despite the large number of works carried out in this field, very few of them are devoted to the quantitative assessment of the marine infragravity wave contribution to elastic vibrations of the upper layer of the Earth's crust. These works are mainly focused on physical formation processes of microseismic noise and its relation to infragravity waves. According to [5], microseismic noise in the range of 80–100 s is related to marine infragravity waves due to the passing storm and is formed by swell waves with a period of 7–10 s. We can note [6] out of few works devoted to the quantitative assessment of the infragravity wave effect on microseismic noise of the Earth's crust. The authors of this work estimated the power of microseismic vibrations caused by a storm in the maximum phase of which microseismic noise reached 1010–1011 J/s. According to [7], 0.9×10^{-7} of energy of marine infragravity waves with a period of 38 s turns into elastic vibrations of the Earth's crust.

This paper quantitatively assesses the influence of bottom pressure due to marine infragravity waves on the upper layer of the Earth's crust and the relationship between the coefficient of bottom pressure transformation into microseismic noise of the Earth's crust and the infragravity wave period.

In August 2018, Typhoon Soulik passed over the Sea of Japan. On the 24th, swell waves generated by the typhoon arrived at the measurement point (Cape Schultz Marine Experimental Station) located on Gamow Island, Peter the Great Bay, Sea of Japan. Arrival of the main wave group was followed by infragravity waves recorded in water and caused microseismic vibrations in the upper layer of the Earth's crust over a wide period range. Both swell and infragravity waves in water were recorded with the help of a laser meter for hydrosphere pressure variations (LMHPVs) [8] installed at a depth of 30 m on the continental shelf from the open part of the Sea of Japan. This device is based on an equal-arm Michelson interferometer,

[a] *Il'ichev Pacific Oceanological Institute, Far East Branch, Russian Academy of Sciences, Vladivostok, 690041 Russia*
**e-mail: ss_budrin@mail.ru*

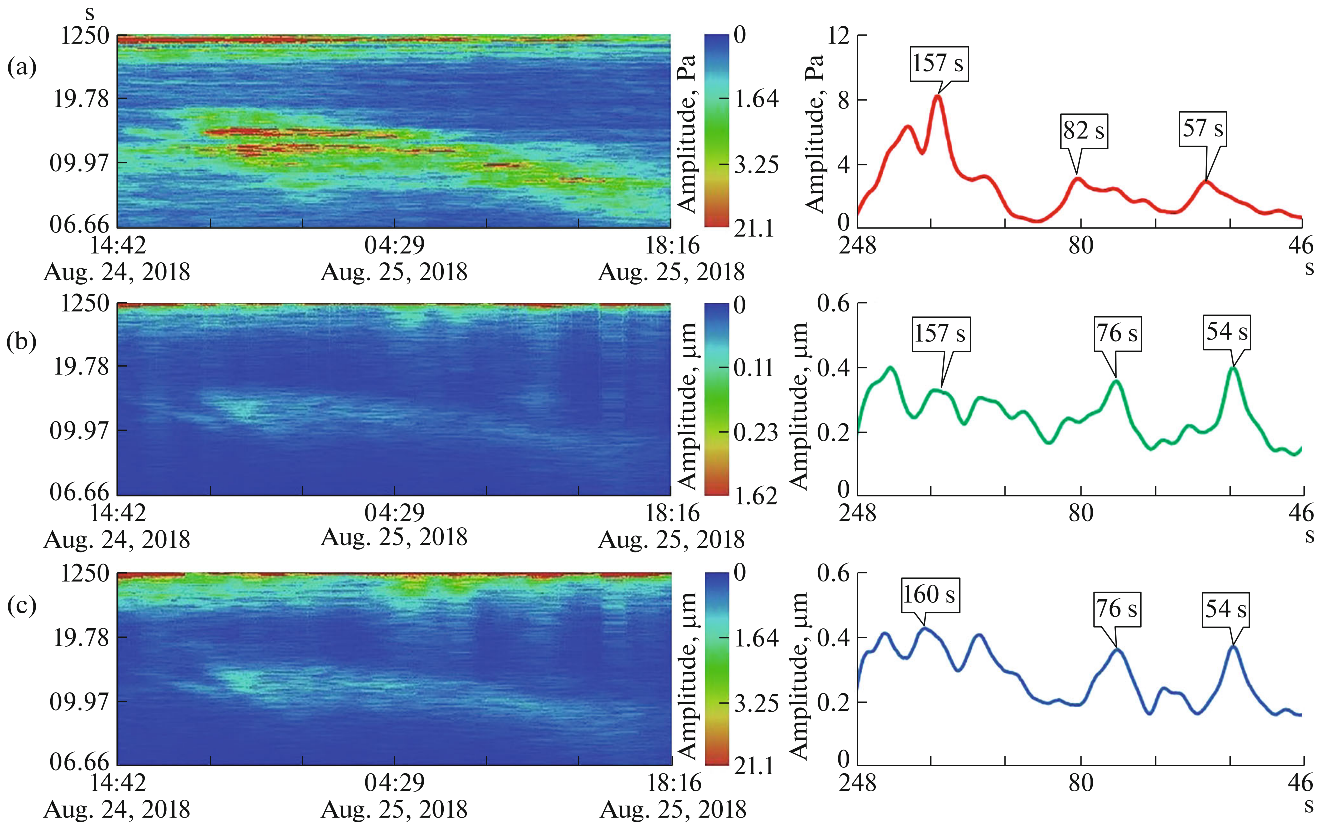

Fig. 1. (a) Spectrogram with arrival of the main swell wave group and infragravity wave spectrum recorded by LMHPV, and (b, c) spectrograms of microseisms of the second type and spectra of microseisms of the first type caused by swell and infragravity waves obtained from the horizontal components of the laser strainmeter North–South 1 and North–South 2.

capable of recording pressure fluctuations in both the infrasound and sound ranges with an accuracy of 1.8 μPa and characterized by a huge dynamic range depending only on the mechanical characteristics of the sensitive element (steel membrane). Hence, it is possible to carry out measurements of multi-scale hydrophysical phenomena in a wide range of amplitudes and periods simultaneously. Microseismic vibrations of the upper layer of the Earth's crust were obtained using a system of two strainmeters: components "North–South 1" and "North–South 2." Both devices are based on an unequal-arm Michelson interferometer, and their measuring arms are 52.5 m long. They are capable of recording the displacement of the Earth's crust with an accuracy of 0.3 nm in the frequency range from 0 (conventionally) to 1000 Hz [9].

Figure 1 shows spectrograms of synchronously recorded swell waves generated by the Soulik typhoon and infragravity wave spectra recorded by all three devices.

The LMHPV spectrogram (Fig. 1a) clearly shows the arrival of the main swell wave group with a period from 14 to 9 s, generated by the typhoon passing over the Sea of Japan. Alongside with that, the spectrogram of strainmeter components, simultaneously with the arrival of swell waves, shows the microseisms of the second type caused by progressive gravity sea waves and observed in the same period range. In addition, with the arrival of swell waves, the record spectra of all devices (Fig. 1) demonstrate the maxima caused by infragravity waves and observed in several period ranges: 160–157, 82–76, and 57–54 s.

As can be seen in the swell wave spectrogram (Fig. 1a), the main wave group is discrete and consists of three components that can be divided into three main period ranges, in particular, 14, 11, and 9 s. If the infragravity and swell wave periods are compared, it turns out that periods of infragravity waves are 11, 7, and 6 times longer than those of the gravity waves that generated them. These data are similar to the research results obtained earlier in this area.

When viewing the spectra recorded (Figs. 1b, 1c), several questions arise. The main one is the reason for the discrepancies in the infragravity wave periods obtained with different devices. This discrepancy is due to variations in the infragravity wave periods over time, as well as in the swell wave periods, and due to the fact that the spectrum was calculated for a segment

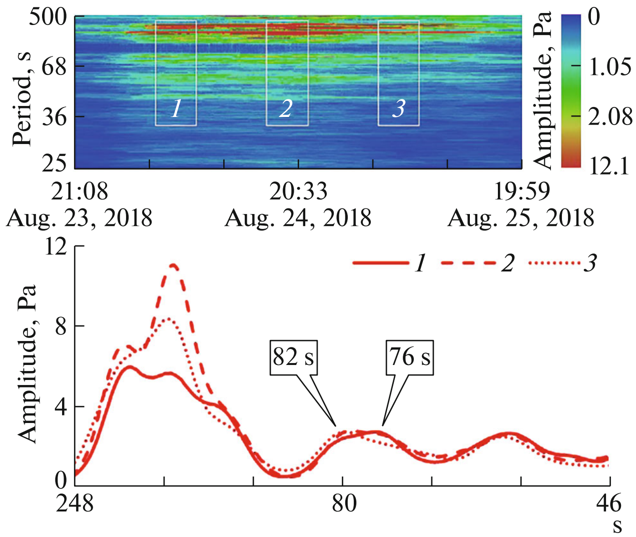

Fig. 2. (a) Infragravity wave spectrogram obtained with LMHPV and (b) spectra constructed from data segments selected in the spectrogram.

of 5 h long, while the entire segment we studied was about a day long. Basically, the differences in periods throughout the study area did not exceed 5 s. The greatest difference in these periods can be seen in the middle harmonic (82 and 76 s). However, when studying the entire area, it can be safely stated that these harmonics are related in the bottom pressure and crustal displacement spectrum, because they appear and disappear simultaneously and depend on each other in terms of amplitude. If changes in the infragravity wave spectrum are considered over time, we can see a slight deviation in the period of the harmonic in question. Figure 2 shows a spectrogram with marked 5-hour intervals used to construct the spectra to demonstrate this period deviation.

In addition, the spectra presented in Figs. 1b and 1c show other common spectral maxima, for example, 207 and 100 s. These maxima were not taken into account in this study, because they were not stationary; they appeared and disappeared throughout the entire time period under study.

For the purpose of the quantitative assessment of transformations of infragravity wave-generated bottom pressure into elastic vibrations of the Earth's crust, spectral amplitude maxima were identified throughout the study area in several period ranges corresponding to the recorded maxima in ten-minute increments. Thus, we can visualize the bottom pres-

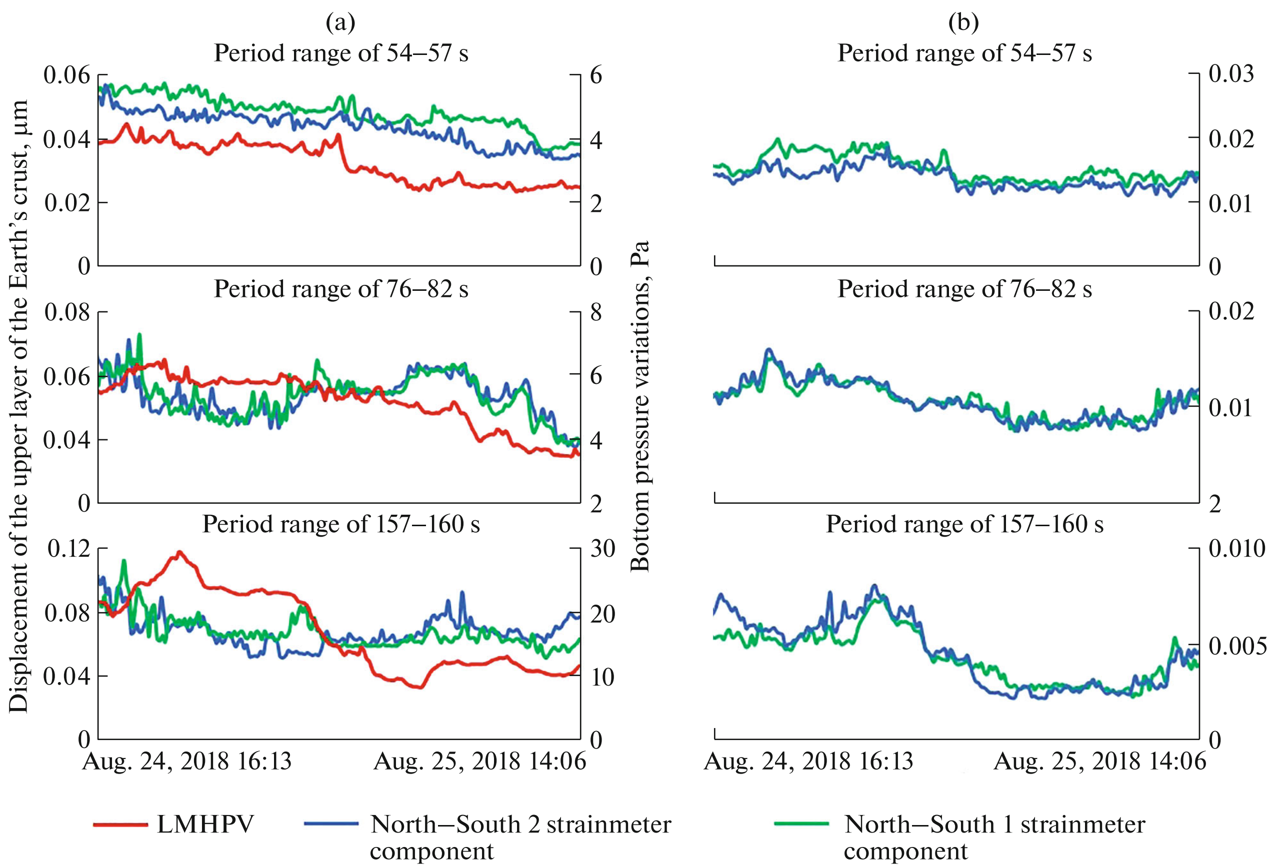

Fig. 3. (a) Amplitude variations in bottom pressure and displacement of the upper layer of the Earth's crust and (b) variations in the transfer coefficient (displacement–bottom pressure ratio) for three period ranges corresponding to those of the recorded infragravity waves.

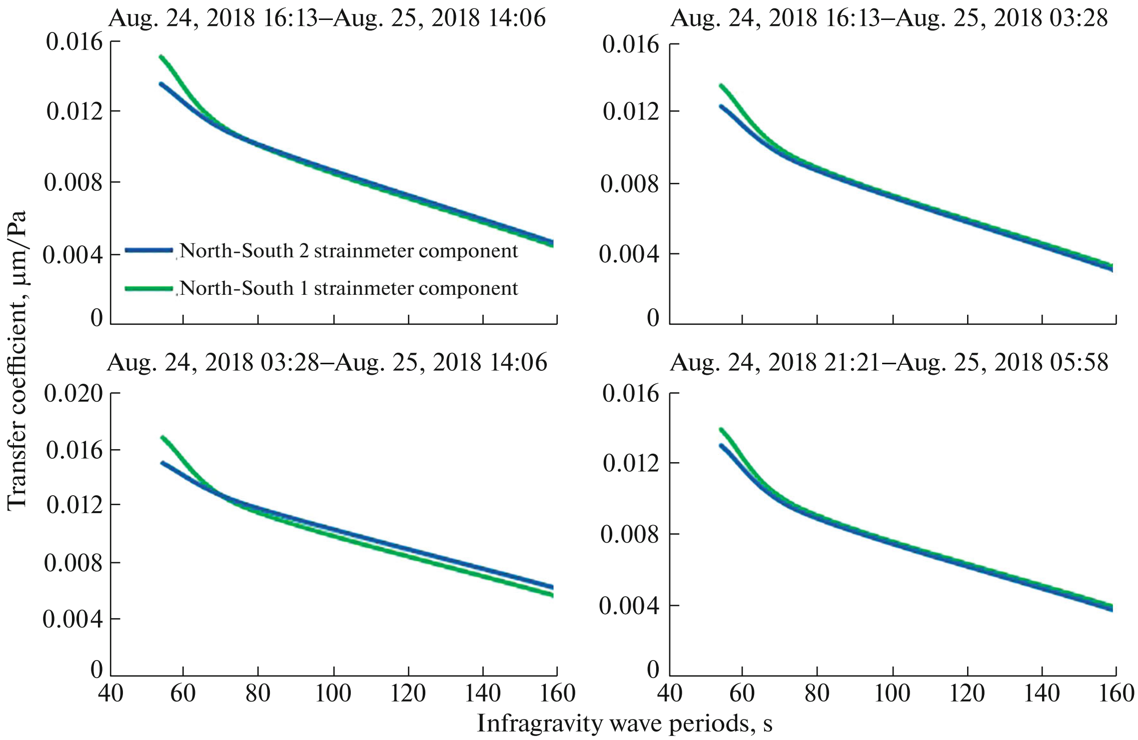

Fig. 4. Dependence of the transfer coefficient on the infragravity wave period for different time intervals.

sure effect on microdisplacements in the Earth's crust, and we can calculate the displacement-to-bottom pressure ratio to quantify this process. As a result, we obtain the transfer coefficient or transformation ratio and its variations over time. Spectral amplitude maxima trends of all devices and transfer coefficient variations are presented in Fig. 3.

When considering Fig. 3a, it can be seen that the variations in the bottom pressure and displacement are almost linear and directly proportional in the period range of 54–57 s and occasionally nonlinear in the higher period ranges. The same nonlinearity, in the same ranges, can be observed in relation to the transfer coefficient (Fig. 2b) defined as the ratio of displacement of the upper layer of the Earth's crust to variations in the bottom pressure. It should be noted that the transfer coefficient values of the North–South 1 and North–South 2 strainmeter components almost coincide and, thus, confirm the processing and calculation correctness, because the devices have the same length of measuring arms and sensitivity and should respond consistently to bottom pressure variations. The nonlinearity discussed above can be explained by the dispersion of swell waves as they propagate from the generation point to the receipt point, if an infragravity wave generation is considered as a swell wave modulation. Initially, the main wave group arrives at the receipt point. Waves with a longer period have a greater amplitude; they create infragravity waves with a period of 157–160 s also characterized by a higher amplitude than other infragravity waves. Over time, waves with a shorter period and lower amplitude begin to arrive at the receipt point and cause amplitude variations in the spectrum of the high-period range toward a decrease. This assumption is confirmed when considering the recorded spectrogram of a laser meter for hydrospheric pressure (Fig. 1a).

Figure 4 shows the relationship between the average transfer coefficient and the period of the infragravity wave.

According to Fig. 4 demonstrating the dependence of the transfer coefficient describing transformations of bottom pressure variations into displacements of the upper layer of the Earth's crust on the infragravity wave period, the transfer coefficient is characterized by a linear monotonic decrease toward an increasing period in the range from 160 to 70 s. However, the periods of 50–70 s are distinguished by a slight nonlinearity which is hard to estimate due to the lack of coefficient values for shorter periods. Figure 3 specifically shows not only the graphs of the entire study area, but also the time intervals located at the beginning, at the end, and in the middle of the main segment. It was done in order to clarify that the amplitude and period variations over time do not affect the transfer coefficient proper.

Hence, it can be concluded that based on the obtained dependences of the transfer coefficient presented in Fig. 3, bottom pressure variations generated by infragravity waves with a period of 160 s, despite their higher amplitude, cause displacements 2–3 times smaller in the upper layer of the Earth's crust than higher variations in the bottom pressure caused by infragravity waves with a shorter period.

FUNDING

This work was supported in part by the Russian Science Foundation (project no. 22-27-00678 "Microdeformations of the Earth's Crust Caused by Infragravity Sea Waves According to the Laser Interference Device Data").

CONFLICT OF INTEREST

The authors of this work declare that they have no conflicts of interest.

REFERENCES

1. F. I. Monakhov, *Low-Frequency Earth's Noise* (Nauka, Moscow, 1977) [in Russian].
2. M. S. Longuet-Higgins, Philos. Trans. R. Soc., A **243** (857), 1–35 (1950). https://doi.org/10.1098/rsta.1950.0012
3. W. H. Munk, Trans. Am. Geophys. Union **30** (6), 849–854 (1949). https://doi.org/10.1029/TR030i006p00849
4. S. C. Webb, Rev. Geophys. **36** (1), 105–142 (1992). https://doi.org/10.1029/97RG02287
5. D. P. Kovalev, G. I. Dolgikh, and G. V. Shevchenko, Dokl. Earth Sci. **461** (2), 368–372 (2015). https://doi.org/10.1134/S1028334X15040030
6. V. N. Tabulevich, V. A. Potapov, E. A. Ponomarev, A. G. Sorokin, and N. N. Drennova, Izv., Atmos. Oceanic Phys. **41** (4), 517 (2005).
7. G. I. Dolgikh and V. V. Ovcharenko, Dokl. Earth Sci. **422** (7), 1129–1133 (2008).
8. G. Dolgikh, S. Budrin, S. Dolgikh, and A. Plotnikov, Sensors **20** (23), 6998 (2020). https://doi.org/10.3390/s20236998
9. G. I. Dolgikh, P. G. Butyrin, S. G. Dolgikh, R. A. Dyagilev, V. A. Shvets, and S. V. Yakovenko, Dokl. Earth Sci. **441** (1), 1583–1587 (2011).

Translated by E. Maslennikova